Phase Equilibrium Diagram of the System Mn–Cr–O

YU. V. GOLIKOV AND V. F. BALAKIREV

Institute of Metallurgy, Ural Science Center, USSR Academy of Sciences, 101 Amundsen St., GSP 812 Sverdlovsk 620219 USSR

A hypothetical oxygen pressure–composition phase diagram and a projection of the oxygen pressure–temperature–composition diagram on the composition triangle were constructed from phase equilibria in the system Mn–Cr–O on the basis of the data available in literature. The temperature–composition phase equilibrium diagram of this same system in air was specified. Isomorphism of solid solutions with spinel and hausmannite structure and their intertransformation was studied. Two chemical compounds, $MnCr_2O_4$ and $Cr_4Mn_{28}O_{48}$, are supposed to exist in the system. © 1987 Academic Press, Inc.

Having compared the data on the system Mn–Cr–O available in literature, a subsolidus portion of the phase equilibrium diagram of the system in air (Fig. 1) (*1*) and the results of a study of phase equilibria during thermal dissociation and reduction with hydrogen of the solid solution $Cr_{1/4}Mn_{11/4}O_4$ to MnO and $MnCr_2O_4$ in the temperature range 800–1000°C (*2*), we made an attempt to draw the P_{O_2}–composition diagram (Fig. 2) and to make the diagram of temperature–composition phase equilibrium in air (Fig. 1) more specific. Figure 2 is not only semiquantitative but also in many ways hypothetical. For lack of experimental data at $P_{O_2} > 10^5$ Pa the upper part of the diagram is constructed by analogy with the diagram of the system in air (Fig. 1). We proceeded from the fact that an increase in O_2 pressure in oxide systems brings about qualitative changes similar to those brought about by a decrease in temperature. The boundaries of regions 1 and 2, 5 and 6, 7 and 7a, as well as

the position of the eutectoid transformation point are, of course, unknown in this case. This is the reason why we have not plotted the O_2 pressure values on the axis at $P_{O_2} > 10^5$ Pa in Fig. 2. The experimental data reported in Ref. (*2*) and the phase boundaries of the system in air at 900°C in accordance with Fig. 1 are marked by solid dots in Fig. 2. To make Fig. 2 less cumbersome, positions of these boundaries at other temperature values are not given. For the same reason we have not plotted the boundaries of regions 1 and 2, 2 and 3, 3 and 4, 4 and 5, 5 and 6, 5 and 7 at 800 and 1000°C. To construct the diagram in Fig. 2 we used the experimental data on phase equilibria in the system Mn–O (*3*), as well as the oxygen pressure values of $MnCr_2O_4$ and Cr_2O_3 dissociation calculated by the method reported in Ref. (*4*) (initial data were taken from Ref. (*5*)).

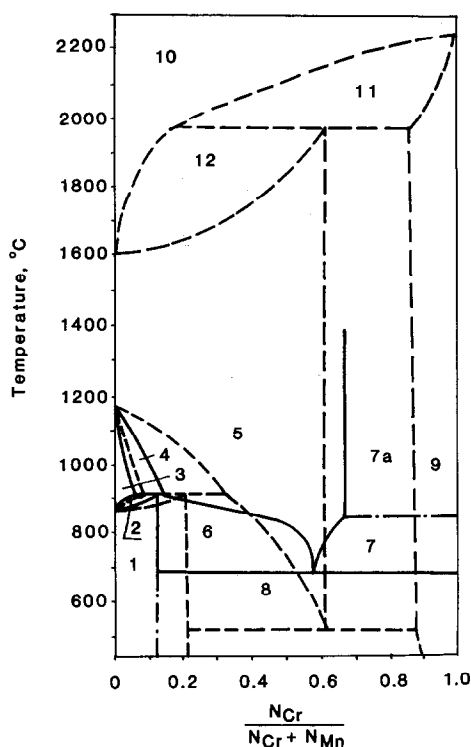The presence of regions 1–8 in Fig. 2 follows from Fig. 1. The position of their

FIG. 1. Phase diagrams of the system Mn–Cr–O in air: solid line represents the phase equilibrium diagram of the system (1), dashed line represents the diagram of water-quenched phases (14), dash-and-dot line represents our results. N_{Cr} and N_{Mn} are atomic fractions of chromium and manganese in the system, respectively. 1, B; 2, B + H; 3, H; 4, H + S; 5, S; 6, B + S; 7, S + Cr$_2$O$_3$; 7a, MnCr$_2$O$_4$ + Cr$_2$O$_3$; 8, B + Cr$_2$O$_3$; 9 according to Ref. (14) is the homogeneity region of solid solution Cr$_c$Mn$_{2-c}$O$_3$ with Cr$_2$O$_3$-type structure (not discovered in Refs. (1) and (15); 10, L; 11, L + Cr$_2$O$_3$; 12, L + S; B is bixbyite, i.e., solid solution with α-Mn$_2$O$_3$-type structure; H is hausmannite structure; S is spinel structure; L is liquid phase.

system are obtained in evacuated silica tubes (1). This is also confirmed by the analogy between a rise in temperature (which gives rise to a leftward shift of region 4 in Fig. 1) and a decrease in oxygen pressure in oxide systems. The slope of the lines bounding region 4 (as well as regions 2, 6, and 7) in Fig. 2 is determined by the laws of geometrical thermodynamics (6). From above and from below region 4 is bounded by horizontal lines (Fig. 2). The upper horizontal corresponds to monovariant equilibrium H + S + B, in accordance with Fig. 1. We dare draw the lower hori-
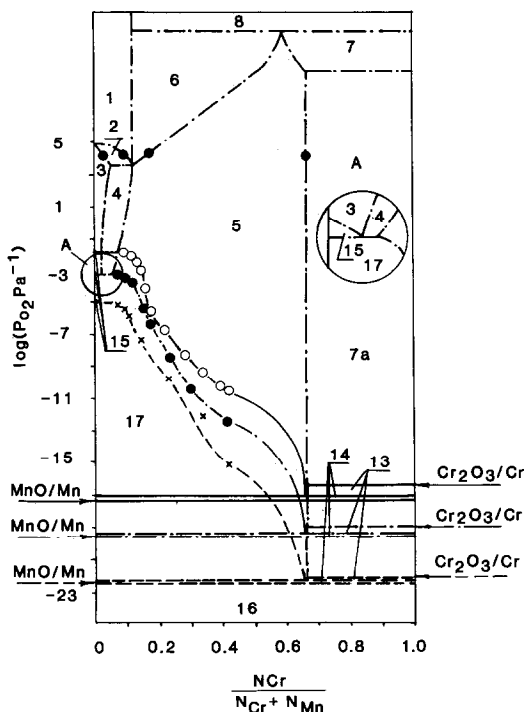

FIG. 2. Hypothetical phase equilibrium diagram of the system Mn–Cr–O at variable oxygen pressure in the gas phase. Solid line, 1000°C; dash-and-dot line, 900°C; dashed line, 800°C: Experimental points: ×, 800°C (2); ●, 900°C (1–2); ○, 1000°C (2). The numbering of phase regions in Figs. 1 and 2 is the same for the sake of comparison. 13, MnCr$_2$O$_4$ + Cr; 14, MnO + Cr, 15, H + MnO; 16, system Mn–Cr; 17, S + MnO.

boundaries in Fig. 2 is arbitrary. The boundaries of region 2 were determined by rough extrapolation of the data reported in Refs. (1, 4). A leftward shift in the boundaries of region 4, which occurs when the oxygen pressure is decreased, follows from a comparison of the experimental data on the system Mn–Cr–O in air with the data generated when the spinel phases of this

zontal because of the similarity of the experimentally obtained oxygen pressure values of dissociation of Mn_3O_4 (3) and the solid solution $Cr_{1/4}Mn_{11/4}O_4$ (2) (Fig. 2). This horizontal can correspond only to equilibrium H + S + MnO. If our assumption is right, region 15 appears inevitably in Fig. 2. Here in equilibrium with the gas phase are MnO and a hausmannite solid solution.

It was experimentally shown in Ref. (2) that the reduction of the solid $Cr_{1/4}Mn_{11/4}O_4$ solution with H_2 + H_2O leads to formation of $MnCr_2O_4$ (spinel) and MnO (manganese protoxide). A further decrease in equilibrium oxygen pressure at the expense of hydrogen desiccation at the temperature of liquid nitrogen does not change the composition of solid products of reduction, and $MnCr_2O_4$ persists until the spinel phase dissociates into metallic chromuim and manganese protoxide, as is shown in Fig. 2. The position of regions 13, 14, and 16 is plotted in accordance with the data reported in Refs. (3–5). At the same time $MnCr_2O_4$ is a boundary composition of region 5 in air at temperatures above 830°C (Fig. 1). We therefore can devide regions 5 and 7a, and 5 and 13 in Fig. 2 by a vertical boundary corresponding to composition $MnCr_2O_4$.

Two specific points corresponding to the boundary compositions of phases with spinel and α-Mn_2O_3-type structures attract our attention: $MnCr_2O_4$ and $Cr_{1/4}Mn_{7/4}O_3$ (or $Cr_4Mn_{28}O_{48}$, taking into account that the unit cell of α-Mn_2O_3 contains 16 formula units). Composition $MnCr_2O_4$ is invariant with respect to temperature (Fig. 1) and oxygen pressure (Fig. 2). $Cr_4Mn_{28}O_{48}$ is invariant with respect to temperature only, since the available experimental data are not sufficient to determine whether it is invariant to oxygen pressure or not. According to Ref. (7), invariance of composition is a sign of the chemical compound. Therefore, proceeding from the equilibrium

phase diagram of the system Mn–Cr–O we can state that there are two chemical compounds in the system: $MnCr_2O_4$ and $Cr_4Mn_{28}O_{48}$. Both of them are chemical compounds in structure too, since "the compound ordinate of the daltonide phase should be regarded as a limiting value of filling certain structural elements in the system of Fyodorov points or a certain part of them" (8, p. 198). In the case of spinel solutions, octahedral sites of $MnCr_2O_4$ allowed in this structure are completely filled with Cr(III) cations and tetrahedral sites with Mn(III) cations (9–13).

In structure (8) $Cr_4Mn_{28}O_{48}$ can also be identified as a chemical compound. Proceeding from the structure of α-Mn_2O_3–$Mn_8(Mn_{24})O_{48}$ we can assume that Cr(III) cations in $Cr_4Mn_{28}O_{48}$ occupy either one-half or one-sixth of the crystallographically nonequivalent sites of the lattice, i.e., they "fill a certain part of structural elements of the system of Fyodorov points," which, according to Ref. (8), permits $Cr_4Mn_{28}O_{48}$ to be classified as a chemical compound decomposing in air at 910 ± 10°C according to the peritectoid reaction (Fig. 1). $MnCr_2O_4$ has the spinel crystal lattice, all A-sites of which are occupied by Mn(II) cations and B-sites of which are occupied by Cr(III) cations. It decomposes in air at 830°C according to a eutectic-type reaction (Fig. 1) with the formation of the solid spinel solution $Mn_xCr_{3-x}O_4$ and chromium oxide Cr_2O_3 (Fig. 1), dissociates according to the peritectoid reaction $MnCr_2O_4$ = MnO + 2Cr + $\frac{3}{2}O_2$ (Fig. 2), and presumably melts in air at about 2000°C. The reason for this assumption is the temperature of peritectic transformation that was detected in the Mn–Cr–O system in air in Ref. (14). Comparing the results of Refs. (1) and (14) (Fig. 1) we can assume that this temperature corresponds to the melting temperature of chemical compound $MnCr_2O_4$. This discrepancy in the diagrams presented in Fig. 1 is due to insufficient time of the synthesis in Ref. (14)

(a detailed analysis of this discrepancy was made in Ref. (*1*)), which may affect the formation of oxide phases. Since samples in Ref. (*14*) were obtained from Mn_2O_3 and Cr_2O_3, initial oxides persisted; i.e., the boundaries of regions 1, 3, and 5 were shifted and region 9 appeared (Fig. 1). Insufficient time of the synthesis could not have affected the position of temperature boundaries of the homogeneity regions of phases with α-Mn_2O_3-type and spinel structures. The point is that formation of even insignificant quantities of $MnCr_2O_4$ and $Cr_4Mn_{28}O_{48}$ inevitably leads to accurate determination of transformation temperatures of these substances. This is confirmed by the coincidence of the upper temperature boundaries of the homogeneity region of the α-Mn_2O_3-type solution (a horizontal line dividing regions 1, 2, and 4 in Fig. 1) in Refs. (*1*) and (*14*).

Having classified $MnCr_2O_4$ and $Cr_4Mn_{28}O_{48}$ as chemical compounds, we divided regions 7 and 7a and prolonged the boundary of region 1 into region 8 (dash-and-dot line in Fig. 1), which was not done in Ref. (*1*). Thus, the anomaly in the position of the boundary between regions 5 and 7 can be explained from the viewpoint of the physico-chemical analysis while it could not be explained within the framework of the structural approach (*1*).

References

1. Yu. V. Golikov, D. V. Bamburov, V. P. Barkhatov, and V. F. Balakirev, *J. Phys. Chem. Solids* **46,** 1357 (1985).
2. A. P. Bobov, A. G. Zalazinsky, V. F. Balakirev, Yu. V. Golikov, and G. I. Chufarov, *Zh. Fiz. Khim.* **58,** 750 (1984).
3. E. K. Kazenas and D. M. Chizhikov, "Pressure and Composition of Vapor over Oxides of Chemical Elements," Nauka, Moscow, (1976).
4. L. P. Vladimirov, "Thermodynamic Calculation of Equilibrium in Metallurgical Reactions," Metallurgiya, Moscow, 1970.
5. Yu. D. Tretyakov, Ph.D. thesis, Moscow University, 1965.
6. A. M. Zakharov, "Equilibrium Phase Diagrams of Binary and Ternary Systems," Metallurgiya, Moscow, 1978.
7. N. S. Kurnakov, "Introduction into Physico-chemical Analysis," Izd. Akad. Nauk USSR, Moscow/Leningrad, 1940.
8. N. N. Sirota, "Physico-chemical Aspect of Phases of Variable Composition," Nauka i Tekhnika, Minsk, 1970.
9. E. W. Gorter, *Philips Res. Rep.* **9,** 295 (1954).
10. S. J. Pickart and R. Natans, *Phys. Rev.* **116,** 317 (1959).
11. J. M. Hastings and L. M. Corliss, *Phys. Rev.* **126,** 556 (1962).
12. Z. Jirak, S. Vratislav, and J. Zajicek, *Phys. Status Solidi A* **37,** 47 (1976).
13. Z. Jirak, S. Vratislav, and P. Novak, *Phys. Status Solidi A* **50,** 21 (1978).
14. D. H. Speidel and A. Muan, *J. Amer. Ceram. Soc.* **46,** 577 (1963).
15. E. Pollert, P. Holba, M. Nevriva, and J. Novak, *J. Phys. Chem. Solids* **38,** 1145 (1977).